



Effective particle magnetic moment of multi-core particles



Fredrik Ahrentorp^a, Andrea Astalan^a, Jakob Blomgren^a, Christian Jonasson^a, Erik Wetterskog^b, Peter Svedlindh^b, Aidin Lak^c, Frank Ludwig^c, Leo J. van IJzendoorn^d, Fritz Westphal^e, Cordula Grüttner^e, Nicole Gehrke^f, Stefan Gustafsson^g, Eva Olsson^g, Christer Johansson^{a,*}

^a Acreo Swedish ICT AB, Arvid Hedvalls backe 4, SE-411 33 Göteborg, Sweden

^b Department of Engineering Sciences, Uppsala University, Box 534, SE-751 21 Uppsala, Sweden

^c Institute of Electrical Measurement and Fundamental Electrical Engineering, TU Braunschweig, D-38106 Braunschweig Germany

^d Department of Applied Physics, Eindhoven University of Technology, 5600 MB Eindhoven, The Netherlands

^e Micromod Partikeltechnologie GmbH, D-18119 Rostock Germany

^f nanoPET Pharma GmbH, D-10115 Berlin Germany

^g Department of Applied Physics, Chalmers University of Technology, SE-412 96 Göteborg, Sweden

ARTICLE INFO

Article history:

Received 30 June 2014

Received in revised form

24 September 2014

Accepted 28 September 2014

Available online 6 October 2014

Keywords:

Magnetic nanoparticles

Magnetic relaxation

Multi-core particles

Single-core particles

ABSTRACT

In this study we investigate the magnetic behavior of magnetic multi-core particles and the differences in the magnetic properties of multi-core and single-core nanoparticles and correlate the results with the nanostructure of the different particles as determined from transmission electron microscopy (TEM). We also investigate how the effective particle magnetic moment is coupled to the individual moments of the single-domain nanocrystals by using different measurement techniques: DC magnetometry, AC susceptibility, dynamic light scattering and TEM. We have studied two magnetic multi-core particle systems – BNF Starch from Micromod with a median particle diameter of 100 nm and FeraSpin R from nanoPET with a median particle diameter of 70 nm – and one single-core particle system – SHP25 from Ocean NanoTech with a median particle core diameter of 25 nm.

© 2014 Elsevier B.V. All rights reserved.

1. Introduction

In biomedical applications where magnetic nanoparticles are used, both magnetic multi-core and single-core particles can be found [1,2]. Magnetic multi-core particles consist of several magnetic single-domain nanocrystals, geometrically positioned in different types of configurations while single-core particles only consist of one single-domain nanocrystal. Depending on the size distribution and configuration of the nanocrystals inside the multi-core particle and the hydrodynamic particle size distribution, different types of magnetic behavior can be obtained. The magnetization process of the magnetic multi-core ensemble will depend on both the individual magnetic moments of the nanocrystals as well as on the total effective magnetic moment of the particle (which in turn depends on both the magnetic moment values and moment orientations of the individual nanocrystals). Magnetic nanocrystals can be coarsely divided into small crystals that show internal magnetic relaxation, Néel relaxation, and larger

crystals with thermally blocked magnetic moment where the nanocrystal magnetic moment is locked in a specific direction in the nanocrystal. If the magnetic nanocrystals are dispersed in a carrier liquid the nanocrystal magnetic moment can be decoupled from the physical particle rotation in the liquid and give rise to Néel relaxation, or the nanocrystal magnetic moment can be physically locked in the nanocrystal. In the latter case, magnetic relaxation occurs at the same rate as the rate of particle rotation in the liquid and gives rise to Brownian relaxation. The parameters that determine whether we have Néel or Brownian relaxation at a given temperature are the size distribution of the nanocrystals, the magnetic material properties (through the magnetic anisotropy), the viscous properties of the liquid and magnetic interactions between the nanocrystals (for instance the interactions between the nanocrystals in a magnetic multi-core particle system). In order to study the magnetic interaction effects in multi-core particles Monte Carlo simulations can be used [3,4]. In these simulations the effects of magnetic interactions between the nanocrystals in the multi-core structure, the nanocrystal size distribution and the magnetic anisotropy can be studied independently from each other. It is seen from these results that in order to

* Corresponding author.

E-mail address: christer.johansson@acreo.se (C. Johansson).

fully understand the magnetic properties of magnetic multi-core particles it is important to include all of these effects.

2. Material and methods

The BNF Starch particles from Micromod are iron oxide based multi-core structured particles with a median particle size of about 100 nm. The particles are prepared by high-pressure homogenization according to the core-shell method [5]. The core of the multiple magnetite nanocrystals is coated with a shell of hydroxyethyl starch. The particles are supplied as suspension in water. The BNF particles are widely used in hyperthermia studies for cancer treatment [6–8] and show interesting properties as contrast agent for magnetic resonance imaging [9]. The FeraSpin R particle system from nanoPET is also an iron oxide multi-core particle system with a median particle size of about 70 nm. The FeraSpin R particles are carboxydextran coated multicore particles, i.e. the multi-core particles consist of clusters composed of smaller nanocrystals of about 5–8 nm [10,11]. The multi-core particles exhibit a size distribution with the smallest one comprising only one nanocrystal per multi-core particle and the larger ones containing multiple nanocrystals per multi-core particle. The Feraspin R multi-core particles are dispersed in water. In the case of the multi-core particles, the particle sizes are defined as the size of the clustered nanocrystals. One major application of FeraSpin R is its use as MRI contrast agent for small animal imaging for pharmaceutical research purposes. The SHP25 particle system from Ocean NanoTech is an iron oxide based single-core particle system (with only one core per particle) with a median particle size of 25 nm. The SHP25 particles are dispersed in water with amphiphilic polymer coating.

In order to study the dynamic magnetic properties, three AC susceptometers were used. The DynoMag system [12] was utilized between 1 Hz and 500 kHz, a lab high frequency AC susceptometer [13] was used in the frequency range between 10 kHz and 10 MHz and an additional lab high frequency susceptometer up to 1 MHz [14]. Measurements were carried out at 300 K.

Magnetization versus field was measured with a MPMS SQUID magnetometer from Quantum Design. The ultra-low field mode utility was used in order to optimize the low field magnetic measurements.

Transmission electron microscopy (TEM) was performed using two different instruments: (1) A FEI Tecnai F20 equipped with a LaB6 electron gun and operated at 200 kV and (2) a FEI Titan 80-300 equipped with a field emission gun and operating at 80 or 300 kV.

3. Results and discussion

In Fig. 1, TEM images of the BNF Starch and FeraSpin R multi-core particle systems and the SHP25 single-core particle system can be seen.

The median value of the multi-core particle size of the BNF Starch particle system is 100 nm with a distribution in diameters of ± 50 nm, by defining circles around the multi-core structures and determining the diameters of these circles. The multi-core particle size is defined as the total size of the clustered nanocrystals (see Fig. 4). An evaluation of 200 multi-core structures was carried out to determine the distribution of the particle sizes. The individual nanocrystal size in the multi-core structure is in the range of 10 nm–20 nm. For the FeraSpin R system the median total particle diameter was determined to be in the range of 70 nm with a distribution in diameters in the range of ± 50 nm and with individual nanocrystal sizes in the range of 5–10 nm. The

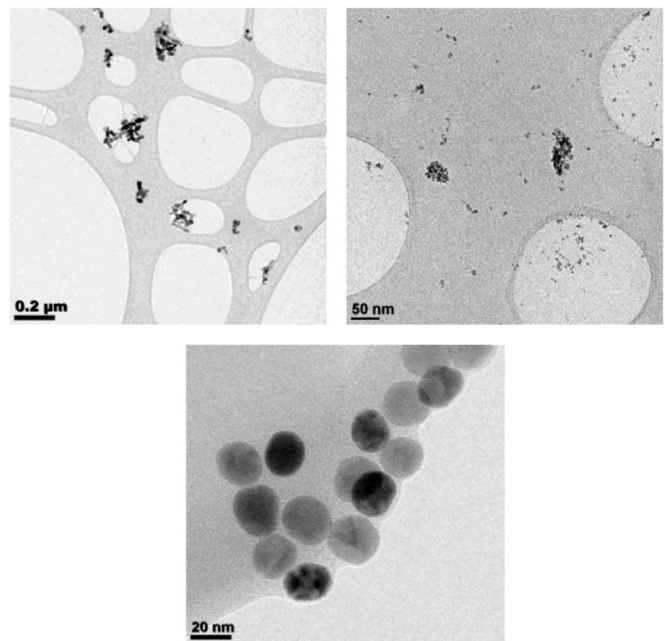


Fig. 1. TEM images showing the BNF Starch (left top) and FeraSpin R (right top) multi-core particles and SHP25 single-core particles (bottom). All particles in the images are dispersed on holey carbon films. In the two upper TEM pictures some of the multi-core structures are shown for the BNF Starch and FeraSpin R particle systems, together with free nanocrystals in the FeraSpin R particle system. Contrast variations among the individual single core particles are due to diffraction contrast in the TEM. The median diameter of the BNF Starch particle system is about 100 nm and 70 nm for the FeraSpin R particle system. The median diameter of the single-core SHP25 particle system is about 25 nm. The clustering of the SHP25 particles as seen in the TEM picture is due to the TEM sample preparation.

determined nanocrystal median diameter of the single-core particle system SHP25 is 25 nm with a distribution in diameters of about ± 5 nm.

In Fig. 2, AC susceptometry data of the three particle systems can be seen. From measurements on dilutions of the samples we found no evidence of interactions between the particles in the dynamic magnetic response (the concentration normalized AC susceptibility curves overlapped and the Brownian relaxation frequencies were constant with particle concentration). Therefore we give the dynamic susceptibility data given in Fig. 2 for the original particle concentrations.

In the AC susceptibility versus frequency data in Fig. 2b we can see three peaks in the imaginary part of the AC susceptibility at 460 Hz for the BNF Starch system, 1 kHz for the FeraSpin R system and 11 kHz for the SHP particle system. As was mentioned in the introduction chapter, magnetic particle systems (multi-core and single-core) can show Brownian or Néel relaxation when they are dispersed in carrier liquid. The type of relaxation depends on particle size parameters (hydrodynamic diameter D_H and nanocrystal diameter D_C), magnetic anisotropy (K), temperature (T) and viscosity (η) of the carrier liquid. From the Brownian relaxation time ($\tau_B = \pi D_H^3 \eta / 2kT$) and the Néel relaxation time ($\tau_N = \tau_0 \exp(K\pi D_C^3 / 6kT)$) where k is the Boltzmann constant and τ_0 the Néel relaxation pre-factor, it is possible to estimate the effective relaxation times for a specific particle system. If we take the BNF Starch system as an example (with $D_H=97$ nm, $D_C=20$ nm, $\eta=10^{-3}$ Pa s, $T=300$ K, $K=2.10^4$ J/m³ and $\tau_0=10^{-9}$ s) we get $\tau_B=346$ μs and $\tau_N=0.6$ s. Due to that $\tau_B < < \tau_N$ the Brownian relaxation will dominate with a relaxation frequency of about 460 Hz ($=1/2\pi\tau_B$) which is the lowest relaxation frequency that can be obtained for this particle system. The same discussion has been carried out for the other two studied particle systems with the conclusion that they also relax substantially via the

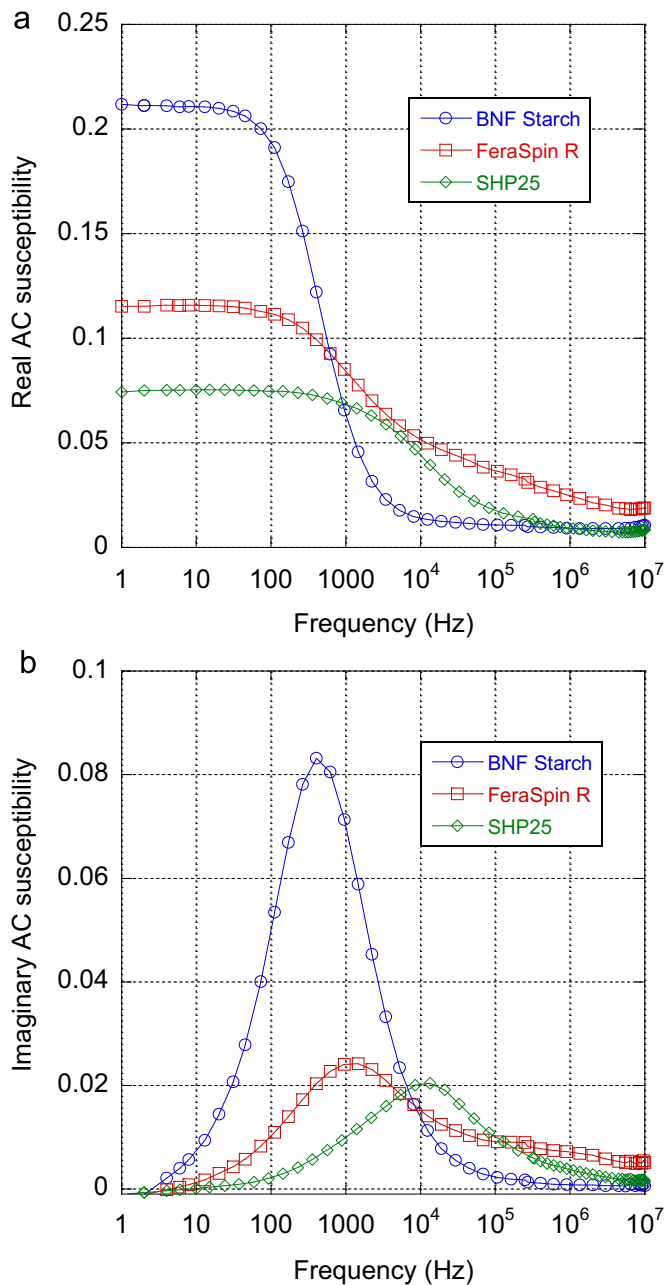


Fig. 2. Real part (a) and imaginary part (b) of the AC susceptibility versus frequency of the three different particle systems. The susceptibilities are given as volume susceptibilities. The AC susceptibility data shown in the figures are for particle concentrations; 24 mg/ml for BNF Starch, 10 mg/ml for FeraSpin R and 4.1 mg/ml for SHP25. The particle concentrations are given as mg particles per ml sample solution. The solid lines through the data points are the results of the fitting procedure described in the text.

Brownian relaxation. The relations above are for the non-interacting case but they give estimates of the order of magnitude of relaxation times. From the AC susceptibility analysis we then conclude that the BNF Starch, FeraSpin R and SHP25 systems exhibit Brownian relaxation frequencies at 460 Hz, 1 kHz and 11 kHz, respectively. From the analysis and modeling of the AC susceptibility data (described below in the text) we find that the BNF Starch system shows only Brownian relaxation, while FeraSpin R exhibits both Brownian relaxation and a contribution from Néel relaxation due to small “free” nanocrystals that exhibit fast relaxations (the free nanocrystals are visible in the TEM images, see Fig. 1). For the BNF Starch particle system above the Brownian relaxation

frequency there is still some high frequency relaxation process (above about 10 kHz) that gives the non-zero value of the real part of the AC susceptibility, see Fig. 2. This high frequency relaxation process is probably due to the intra-potential-well contribution of the single-domain nanocrystals to the AC susceptibility [13,16]. The Néel relaxation contribution to the AC susceptibility for the FeraSpin R particle system can best be seen in Fig. 2 as “shoulders” in the imaginary part of the AC susceptibility spectra at frequencies around 300 kHz for the FeraSpin R and SHP25 particle systems.

By using different AC susceptibility models based on Debye relations for multi-core and single-core particles integrated over a size distribution (log-normal distribution) considering both Brownian and Néel relaxation behavior [12–15] and fitting the AC susceptibility data to these models, we are able to determine the particle and nanocrystal (core) size of the particle systems. The determined particle size from the AC susceptibility analysis is largely dependent on the surrounding liquid (that is the viscosity of the carrier liquid) while the determined nanocrystal (core) size is largely dependent on the nanocrystal intrinsic magnetic anisotropy. From the results of the fitting procedures we are also able to determine the proportion of Brownian relaxation in relation to Néel relaxation in the AC susceptibility response. The results of the particle and core size determinations from the AC susceptometry analysis are summarized in Table 1 and the result of the fitting procedure can be seen as solid lines in Fig. 2. The determined particle sizes from the AC susceptometry analysis are comparable to sizes determined from TEM and dynamic light scattering (DLS) data (data given in Table 1). The determined nanocrystal sizes differ from the sizes determined from the TEM pictures for the multi-core particles. The determined nanocrystal sizes are somewhat lower for the BNF Starch system and much larger for the FeraSpin R system, which is probably due to neglecting magnetic interaction effects between the nanocrystals in the multi-core structures in the used models. For the SHP25 particle system both the particle and core size are comparable to the TEM images. The difference between the particle and core size is due to the particle coating.

Further, from the DC susceptibility determined from the fitting result and only consider the parts of the AC susceptibility models that are dependent on the Brownian relaxation, we can determine the blocked effective magnetic moment of the particles. These blocked effective magnetic moments follow the particle rotations and is responsible for the Brownian relaxation that is seen in Fig. 2. The value of the effective particle moment, μ_{eff} , can be determined

Table 1

Compilation of the magnetic particle AC susceptometry size analysis and the estimated effective particle magnetic moments, μ_{eff} , determined from the AC susceptometer analysis and Eq. (1). In the last two columns to the right the magnetic moments of the individual nanocrystals, μ_C , and the effective magnetic particle moment divided by the magnetic moment of the nanocrystals are shown. The determination of μ_C is explained in the text below Table 1. The hydrodynamic sizes as determined from DLS analysis are 97 nm for BNF Starch, 66 nm for the FeraSpin R system and 25 nm for the SHP25 system.

Particle system	Type	Particle and core median sizes (nm)	$\mu_{\text{eff}} (10^{-18} \text{ Am}^2)$	$\mu_C (10^{-18} \text{ Am}^2)$	μ_{eff}/μ_C
BNF Starch	Multi-core	97 (particle) and 12 (core)	11.9	0.7	17
Fera Spin R	Multi-core	69 (particle) and 14 (core)	6.5	0.1	65
SHP25	Single-core	35 (particle) and 20 (core)	3.1	3.4	0.9

by using the low field expansion of the Langevin expression:

$$\chi_{OB} = \mu_0 n \frac{\mu_{eff}^2}{3kT} \quad (1)$$

where χ_{OB} is the DC susceptibility due to the Brownian relaxation, μ_0 the permeability of vacuum and n number of particles per unit volume (determined from the particle concentration given in mg/ml and the particle or core volume of the particle ensemble as determined from the TEM analysis). In Eq. (1) magnetic interactions between the particles are neglected.

The determined particle sizes (of the multi-core particle systems), nanocrystal (core) size (for the single-core particle systems) and the values of the effective magnetic moment for each of the three particle systems, can be seen in Table 1.

In Table 1, μ_c is the magnetic moment of the nanocrystals ($=M_S V$, where V is the nanocrystal volume determined from the TEM analysis and M_S is the intrinsic saturation magnetization). $M_S = 370$ kA/m (BNF Starch), 350 kA/m (FeraSpin R) and 430 kA/m (SHP25) determined from the high field magnetization data at 300 K (not shown).

Magnetization versus field measurements at 300 K (above the melting temperature of the carrier liquid) of the three investigated particle systems can be seen in Fig. 3.

In a multi-core particle containing several nanocrystals the individual magnetic moments of the nanocrystals add up vectorially to form the effective particle magnetic moment, see Fig. 4.

If the individual nanocrystal moments in the multi-core particle are thermally blocked with respect to the time scale of the physical rotation of the particle (that is the Néel relaxation time is longer than the Brownian relaxation time, $\tau_N > \tau_B$, as discussed earlier in the text in connection to Fig. 2) the effective particle moment will be blocked along a specific direction. In this case the effective particle moment rotates with the same rate as the particle itself and the particle ensemble relaxes via the Brownian relaxation mechanism, which is the case for all of the BNF Starch particles and a fraction of the FeraSpin R particles. In the case of the single-core nanoparticle system, SHP25, the majority of the nanocrystals exhibit Néel relaxation times that are longer than the Brownian relaxation time of the particles ($\tau_N > \tau_B$) and also show Brownian relaxation behavior. In the Feraspin R and SHP25 particle systems there are also some Néel relaxation that contributes to the measured AC susceptibility. This is discussed in connection to Fig. 2.

For the single-core nanoparticle system (SHP25) the value of the effective particle magnetic moment and the nanocrystal magnetic moment is very similar (see Table 1), which is expected since there is only one nanocrystal per particle. There is a small difference between the two values and this is due to measurement and analysis errors in the two used methods to determine the effective particle moment (AC susceptometry and magnetization versus field measurements at high fields) and also that the two methods probe somewhat different magnetic moments when there is a size distribution. For the multi-core particle systems (BNF Starch and FeraSpin R) these two magnetic moments are not equal (see Table 1). If the nanocrystals in the multi-core structure are assumed to have the same magnetic moment μ_c and to be magnetically non-interacting one would expect that the effective particle magnetic moment will follow the statistical relation for randomly oriented independent (non-interacting) nanocrystal magnetic moments according to

$$\mu_{eff} = \mu_c \sqrt{N} \quad (2)$$

where N is the number of nanocrystals in the multi-core structure. In order to estimate values of N we assume a nanocrystal volume packing fraction ratio in the multi-core structure of about 50% and

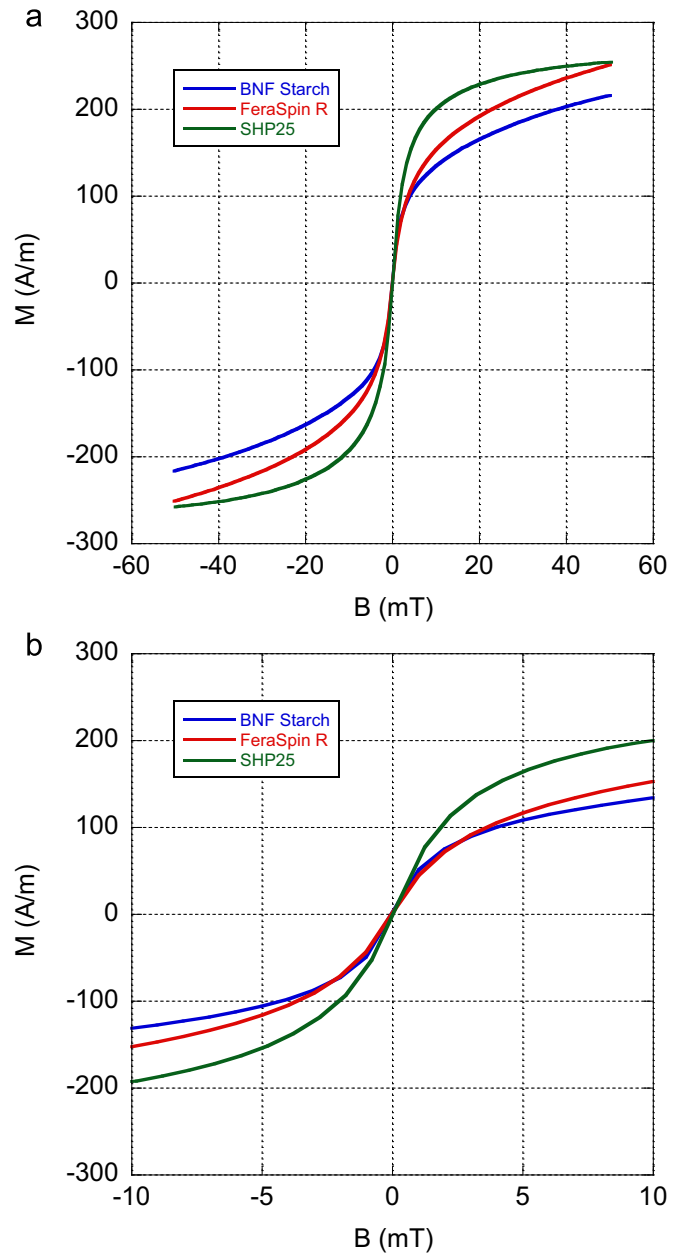


Fig. 3. Magnetization versus field in the range of ± 50 mT (a) and a close up view in the field range of ± 10 mT (b) at 300 K for BNF Starch, FeraSpin R and SHP25. The particle concentration of the studied particle systems was 6.9 mg/ml, except for the SHP25 particle system with a particle concentration of 4.1 mg/ml. Even if the nanocrystal sizes are not exactly the same between the studied particle systems the differences in the magnetization processes of the multi-core and single-core behavior are clearly seen. The intrinsic saturation magnetization is 370 kA/m for the BNF Starch system, 350 kA/m for the FeraSpin R system and 430 kA/m for the SHP25 system, determined from the high field magnetization data at 300 K (not shown).

use the values of the particle and nanocrystal sizes as determined from the TEM analysis. If we do this we find that the ratio of μ_{eff} and μ_c using Eq. (2) is about 12 for the BNF Starch system (using $N=150$) and about 18 for the FeraSpin R system (using $N=330$). The magnetic moment ratio value is in the same range for the BNF Starch but not for the FeraSpin R system, see Table 1. Even if we assume a higher packing fraction of 74% (hexagonal close packed) which gives a ratio value of 22, it is not close to the value for Feraspin R as given in Table 1. In order to obtain the moment ratio of 65 we need in the range of 4000 nanocrystals per particle for the FeraSpin R system which is unrealistic. From this we can

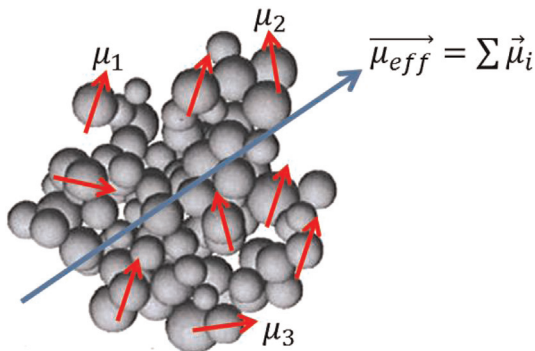


Fig. 4. Schematic picture of a multi-core particle. The figure shows the effective particle moment, μ_{eff} , which is equal to the vector sum of all nanocrystal magnetic moments, μ_i in the particle. Only some of the nanocrystal magnetic moments are shown. The multi-core particle sizes given in the text is defined as the total size of the clustered nanocrystals.

conclude that the magnetic interactions between the nanocrystals in the multi-core structures for the BNF Starch system are weaker than for the FeraSpin R system. The result also implies that the magnetic interactions cause the nanocrystal moments in the FeraSpin R multi-core system to be more aligned with respect to each other compared to random oriented nanocrystal moments. The higher magnetic interaction effect in the FeraSpin R system can also be seen by comparison of the size analysis of the nanocrystals from AC susceptometry, see Table 1 and the size values determined from the TEM pictures. The nanocrystal sizes from the AC susceptometry size analysis are closer to the values determined from the TEM pictures for the BNF Starch system compared to the ACS and TEM size analysis for the FeraSpin R system. In our modeling of the AC susceptometry spectra we have not yet included the effects of magnetic interaction in the magnetic multi-core structures. This will be one of the future tasks, to fully account for the magnetic interactions in the magnetic models. The nanocrystals in the FeraSpin R particle system are more densely packed than for the BNF Starch system (which can be seen from Fig. 1). This will give a larger magnetic interaction effect in the FeraSpin R system compared to the BNF Starch system.

The difference in the magnetic behavior between multi-core and single-core particles can also be seen in the magnetization versus field data, cf. Fig. 3. The particle concentration is almost the same and the measured sample magnetic moment is normalized to the sample volume. As can be seen the magnetization increase with field in the low field region is almost the same for all particle systems (i.e. the particle systems almost exhibit same low field susceptibility, which is in agreement with the AC spectra shown in Fig. 2). We can also see in Fig. 3 that when the field increases the magnetization increases faster for the single-core particle system as compared with the magnetization for the multi-core particle systems. This can be explained by that at low field the magnetization of the multi-core particle systems is dominated by the partial alignment of the effective magnetic moment along the field direction and at higher fields the individual nanocrystal magnetic moments in the multi-core structure become aligned along the field direction which is “hindered” by the magnetic anisotropy in the nanocrystals and thereby the magnetization increase is smaller than for the single-core particle systems. For the single-core nanoparticles the nanocrystals can physically rotate and are not “hindered” by the magnetic anisotropy of the nanocrystals, which increase the magnetization.

The initial susceptibility of the particle systems as shown in Fig. 3 is almost the same for the three particle systems despite the fact that the effective magnetic moments are different, cf. Table 1.

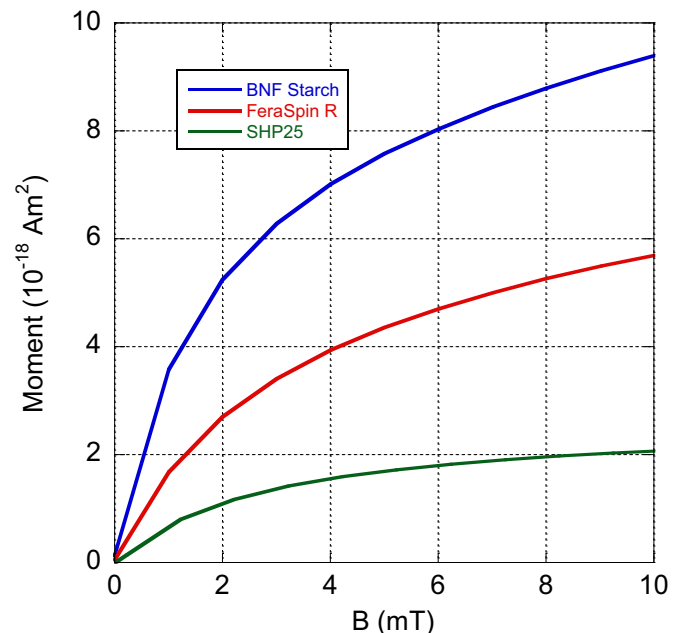


Fig. 5. Magnetic moment versus field for BNF Starch, FeraSpin R and SHP25. The measured sample magnetic moments were normalized with the number of particles per unit volume, taking into account only the blocked magnetic moments of the FeraSpin R particle system. By normalizing in this way the magnetic moment reflects the mean value of the of the particle magnetic moment projected onto the field direction.

This is due to the fact that the number of single-core particles (SHP25) per unit volume is larger than for the multi-core particle systems (BNF Starch and FeraSpin R) and also that the FeraSpin R system has a contribution from particles that exhibit Néel relaxations, which is a superparamagnetic contribution to the magnetization versus field measurements. The superparamagnetic Néel contribution can be distinguished from the Brownian contribution in the AC susceptometry analysis. If the low field magnetization curves are normalized with the number of particles per unit volume and for the FeraSpin R particle system if also the Néel relaxation contribution is removed from the magnetization, we get the magnetization versus field curves shown in Fig. 5.

In Fig. 5 we can clearly see the difference in the magnetization at low fields that is due to the differences in the effective particle magnetic moments.

4. Conclusions

For the studied multi-core particle systems BNF Starch and FeraSpin R, the effective particle magnetic moment of the multi-core particle system is affected by magnetic interactions between the nanocrystals that build up the multi-core particles. The effect of the interactions between the nanocrystals in the multi-core particles is larger for the FeraSpin R system compared to the BNF Starch system. In the FeraSpin R multi-core particle system we have many more nanocrystals (but smaller in nanocrystal size) and more densely packed nanocrystals compared to the BNF Starch multi-core system. We are now working with a Monte-Carlo model to further explain and understand this situation in detail.

Even if the sizes of the individual nanocrystals are not exactly the same for the studied particle systems, the different magnetization behavior can be seen in both the magnetization versus field curve as well as in the AC susceptometry data, which is due to the formation of a blocked effective magnetic moment in the multi-core structured particles.

As shown here, by combining different analysis techniques, AC susceptometry together with magnetization versus field measurements and TEM and DLS data, the degree of magnetic interactions in magnetic multi-core particles can be determined, by studying the result of size analysis using the different methods.

Acknowledgements

The work in this study is financed from the EU FP7 NMP Project NanoMag Grant agreement no: 604448.

References

- [1] Q.A. Pankhurst, J. Connolly, S.K. Jones, J. Dobson, Applications of magnetic nanoparticles in biomedicine, *J. Phys. D: Appl. Phys.* 36 (2003) 167–181.
- [2] K.M. Krishnan, Biomedical nanomagnetics: a spin through possibilities in imaging, diagnostics, and therapy, *IEEE Trans. Magn.* 46 (2010) 2523–2558.
- [3] V. Schaller, G. Wahnström, A. Sanz-Velasco, S. Gustafsson, E. Olsson, P. Enoksson, C. Johansson, Monte Carlo simulation of magnetic multi-core nanoparticles, *J. Magn. Magn. Mater.* 321 (2009) 1400–1403.
- [4] V. Schaller, G. Wahnström, A. Sanz-Velasco, P. Enoksson, C. Johansson, Effective magnetic moment of magnetic multi-core nanoparticles, *Phys. Rev. B* 80 (2009) 092406-1–092406-4.
- [5] J. Teller, F. Westphal, C. Grüttner, Magnetic Nanoparticles with Improved Properties, WO 2005006356, 2005.
- [6] C. Dennis, A.J. Jackson, J.A. Borchers, P.J. Hoopes, R. Strawbridge, A.R. Foreman, J. Van Lierop, C. Grüttner, R. Ivkov, Nearly complete regression of tumors via collective behavior of magnetic nanoparticles in hyperthermia, *Nanotechnology* 20 (39) (2009) 395103.
- [7] D.E. Bordelon, C. Cornejo, C. Grüttner, F. Westphal, T.L. DeWeese, R. Ivkov, Magnetic nanoparticle heating efficiency reveals magneto-structural differences when characterized with wide ranging and high amplitude alternating magnetic fields, *J. Appl. Phys.* 109 (12) (2011) 124904.
- [8] M. Hedayati, T. Owen, B. Abubaker-Sharif, H. Zhou, C. Cornejo, Y. Zhang, M. Wabler, J. Mihalic, C. Grüttner, F. Westphal, A. Geyt, T.L. DeWeese, R. Ivkov, The effect of cell-cluster size on intracellular nanoparticle-mediated hyperthermia: is it possible to treat microscopic tumors, *Nanomedicine* 8 (1) (2012) 29–41.
- [9] M. Wabler, W. Zhu, M. Hedayati, A. Attaluri, H. Zhou, J. Mihalic, A. Geyh, T. L. DeWeese, R. Ivkov, D. Artemov, Magnetic resonance imaging contrast of iron oxide nanoparticles developed for hyperthermia is dominated by iron content, *Int. J. Hyperth.* 30 (3) (2014) 192–200.
- [10] F. Ludwig, T. Wawrzik, T. Yoshida, N. Gehrke, A. Briel, D. Eberbeck, M. Schilling, Optimization of magnetic nanoparticles for magnetic particle imaging, *IEEE Trans. Magn.* 48 (2012) 3780–3783.
- [11] A. Gehrke, F. Briel, H. Ludwig, T. Remmer, Wawrzik, S. Wellert, New perspectives for MPI: a toolbox for tracer research, in: *Magnetic Particle Imaging a Novel SPIO Nanoparticle Imaging Technique*, in: T.M. Buzug, J. Borgert (Eds.), Springer Proceedings in Physics, vol. 140, Springer, Berlin Heidelberg, 2012, pp. 99–103, pp..
- [12] A.P. Astalan, C. Jonasson, K. Petersson, J. Blomgren, D. Ilver, A. Krozer, C. Johansson, Magnetic response of thermally blocked nanoparticles in a pulsed magnetic field, *J. Magn. Magn. Mater.* 311 (2007) 166–170.
- [13] F. Ahrentorp, A.P. Astalan, C. Jonasson, J. Blomgren, B. Qi, O.T. Mefford, M. Yan, J. Courtois, J.-F. Berret, J. Fresnais, O. Sandre, S. Dutz, R. Müller, C. Johansson, Sensitive high frequency AC susceptometry in magnetic nanoparticle applications, *AIP Conf. Proc.* 1311 (2010) 213–223.
- [14] F. Ludwig, A. Guillaume, M. Schilling, N. Frickel, A.M. Schmidt, Determination of core and hydrodynamic size distributions of CoFe₂O₄ nanoparticle suspensions using ac susceptibility measurements, *J. Appl. Phys.* 108 (2010) 033918-1–033918-5.
- [15] F. Öisjöen, J.F. Schneiderman, A.P. Astalan, A. Kalabukhov, C. Johansson, D. Winkler, A new approach for bioassays based on frequency- and time-domain measurements of magnetic nanoparticles, *Biosens. Bioelectron.* 25 (2010) 1008–1013.
- [16] P. Svedlindh, T. Jonsson, J.L. Garcia-Palacios, Intra-potential-well contribution to the AC susceptibility of a noninteracting nano-sized magnetic particle system, *J. Magn. Magn. Mater.* 169 (1997) 323–334.